EurJOC
European Journal of Organic Chemistry

Research Article
doi.org/10.1002/ejoc.202201289

Chemistry Europe
European Chemical Societies Publishing

www.eurjoc.org

Special Collection

Mechanistic Studies on the Bidentate Lewis Acid Catalyzed Domino Inverse Electron-Demand Diels-Alder/Thiol Transfer Reaction

Sebastian Beeck[a] and Hermann A. Wegner*[a, b]

Recently, we presented a novel enantioselective multicomponent reaction of phthalazines, aldehydes and thiols accessing thioether-substituted 1,2-dihydronaphthalenes. Herein, a comprehensive investigation on the mechanism of this domino inverse electron-demand (IEDDA)/thiol transfer reaction is disclosed. In particular, the origin of the stereochemical outcome has been rationalized, as well as structural requirement of the thiol component for an efficient transfer step. Detailed NMR spectroscopy studies uncover a competing reaction pathway resulting in *N,S*-acetals. In addition, DFT computations illuminate the mechanism of the group transfer process and enable an explanation for the formation of the most dominant by-product. The insights allow a direct prediction of suitable substrates for the reaction and provide the basis for further developments of novel stereoselective domino reactions.

Introduction

Efficiency is one key aspect for evaluating a synthesis route and in particular the number of steps involved - referred to as step economy. Each additional synthesis step reduces the overall yield, consumes further energy and resources, and requires time[1] and effort. The incorporation of multicomponent reactions (MCRs) into a synthetic strategy represent an appealing way to meet the demand for short synthesis routes, as they can be used to build up versatile structures in a single step.[2] Their capability has been demonstrated in countless drug and total syntheses.[3] Moreover, MCRs open up access to a whole range of biologically active substances.[4] In the past, we incorporated the bidentate Lewis acid catalyzed inverse electron-demand Diels-Alder (IEDDA) reaction in various domino processes combining diazenes, aldehydes and amines in efficient MCR processes.[5] Recently, we presented an enantioselective, three-component reaction, which gives preparative access to so far unexplored thioether substituted *trans*-1,2-dihydronaphtalenes (**4**) (Scheme 1).[6] In this method simple and readily available phthalazine (**1**), an aldehyde **2** and a thiol **3** were subjected to a tandem catalyzed inverse electron-demand Diels-Alder (IEDDA) reaction. Phthalazine (**1**) is activated by the bidentate Lewis acid 9,10-dimethyl-9,10-diboraanthracene (Me_2-DBA, **5**) for the IEDDA step with an in situ formed enamine. The absolute stereochemistry is controlled by a newly developed chiral amine catalyst **6a**.

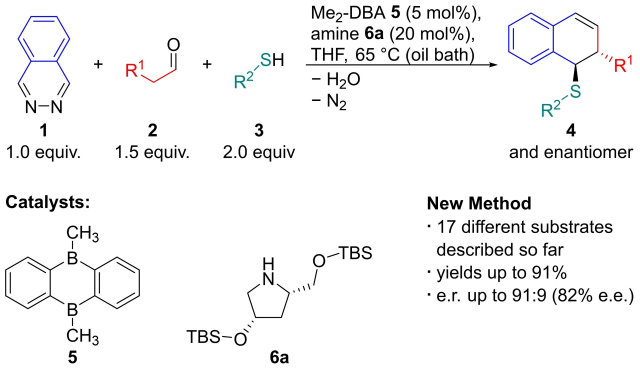

Scheme 1. Multicomponent process between phthalazine (**1**), an aldehyde **2** and a thiol **3** enabling efficient access to the library of thioether substituted *trans*-1,2-dihydronaphthalenes **4**.

Although a preliminary mechanism has been proposed in our initial study, detailed investigations have not been done. Open questions are: How does the chirality of the catalyst translate into the product? Why are electron rich thiols not effective in the transformation, although they should exhibit the higher nucleophilicity? What is the reason for the long reaction times in comparison to the very similar domino IEDDA-amine transfer reaction? In order to clarify these issues, we separately investigated the individual stages of the overall reaction sequence by NMR experiments and DFT computations. The first stage is the formation of the dienophile and diene, which is marked by a network of equilibria and the most dominant ones are now identified. Next, the IEDDA step has

[a] *S. Beeck, Prof. Dr. H. A. Wegner*
Justus Liebig University Giessen
Institute of Organic Chemistry
Heinrich-Buff-Ring 17, 35392 Giessen (Germany)
E-mail: Hermann.A.Wegner@org.chemie.uni-giessen.de
[b] *Prof. Dr. H. A. Wegner*
Justus Liebig University Giessen
Center for Materials Research (ZfM/LaMa)
Heinrich-Buff-Ring 16, 35392 Giessen (Germany)

Supporting information for this article is available on the WWW under https://doi.org/10.1002/ejoc.202201289

Part of the joint "Boron Chemistry" Special Collection.

Research Article
doi.org/10.1002/ejoc.202201289

been addressed focusing on the transition states to rationalize the observed enantioselectivity. Finally, the details of the group transfer reaction have been looked at, especially studying the nature of the applied thiol.

Mechanistic Proposal

We have demonstrated in multiple examples, that Me_2-DBA **5** is a suitable bidentate Lewis acid (BiLa) to activate phthalazines in IEDDA reactions with enamines.[7] Enamines are also key intermediates in various organocatalytic transformations, where enantioselectivity is established by chiral secondary amines.[8] The IEDDA/group transfer domino process investigated in this study combines the BiLa activation of phthalazine with the asymmetric feature of organocatalysis. Our proposed orthogonal mechanism[9] starts with the activation of phthalazine (**1**) by complexation with LA catalyst **5** (Scheme 2).[10] In this complex, the LUMO level is lowered to endorse the [4+2] cycloaddition with enamines under moderate conditions.[11] In parallel, an aldehyde **2** and chiral secondary amine **6** generate the dienophile, the chiral *trans*-enamine **7**. Enamine **7** and complex **A** pass through the central IEDDA reaction to give intermediate **B**. The chiral elements at the amine determine the spatial arrangement between diene and dienophile, which defines the stereochemistry in this method. Subsequently, LA catalyst **5** is recovered and nitrogen is cleaved from DA product **B**, leaving the *o*-quinodimethane intermediate **C**. At this point in the reaction sequence, thiol **3** undergoes a group exchange reaction with intermediate **C** while the amine catalyst **6** is released. Simultaneously, aromaticity is re-established and the final thioether-1,2-dihydronaphthalene product **4** is formed.

The entire mechanism can be divided in three sections: First the generation of the electron-deficient diene and electron-rich dienophile, then, the IEDDA reaction itself and finally, the concluding group transfer reaction. These three parts were studied separately.

Methods

NMR Studies

Air sensitive NMR samples were prepared in a glovebox under inert conditions. Proton NMR (^{1}H NMR) measurements were used to study reaction equilibria in solution and to detect long-lived intermediates. In addition, the progress of the reaction was followed by NMR spectroscopy. For this purpose, samples of the reaction solution were taken, from which the volatile components were removed, the residues re-dissolved in a deuterated solvent and the NMR spectra measured. In this way, it was checked, for example, whether the phthalazine had been completely converted.

Computational Studies

Initial geometries were optimized utilizing the M06-2x functional and def2-tzvpp basis sets (1 atm, 335 K). Previous studies proofed the M06-2x functional as especially reliable.[12] Additionally, the method reproduces well the asynchronous bond formation processes in DA reactions.[13] A triple-ζ basis set with two sets of polarization functions was picked, because polarizable third row elements, namely silicon and sulfur, are involved in the reaction. It was expected that non-covalent interactions (NCIs) have a significant impact on the course of the reaction. One option to account for this effect in DFT optimizations is to incorporate empirical dispersion corrections (e.g. developed by Grimme and coworkers).[14] However, the M06-2x functional benefits little from this correction,[12b,15] due to the way it is parametrized. Optimizations were complemented by frequency computations to check that there are no imaginary frequencies in ground states and solely one coherent imaginary frequency in transition states. Transition states were also related to ground states by intrinsic reaction coordinate (IRC) plots. Furthermore, single point energy values of the DFT optimized geometries were refined by DLPNO-CCSD(T)/def2-

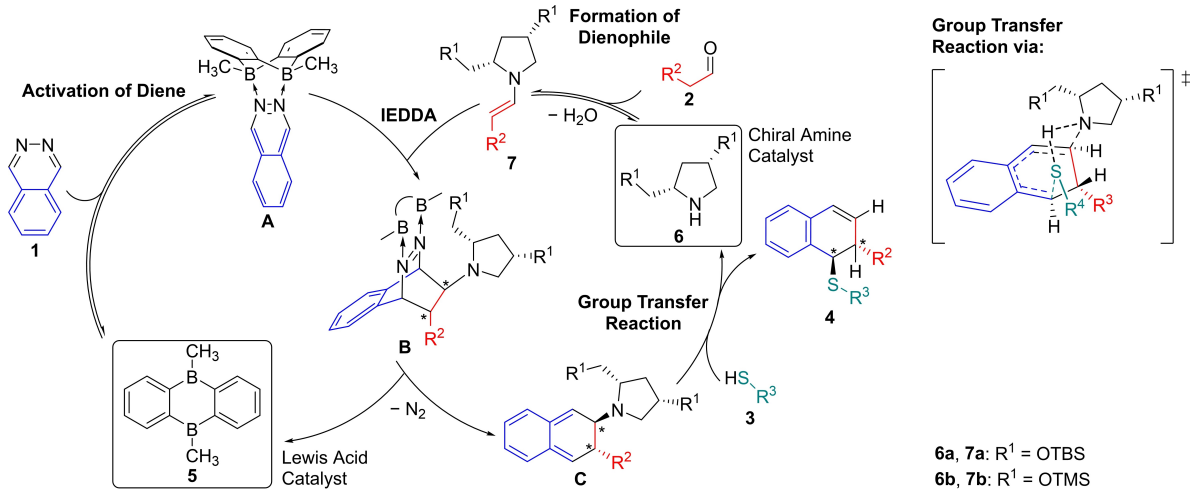

Scheme 2. Mechanistic proposal of the enantioselective IEDDA/group transfer reaction.

Research Article
doi.org/10.1002/ejoc.202201289

tzvpp computations. Frontier molecular orbitals were illustrated on wB97x-D/cc-pVTZ computational method.

Results and Discussion

Formation of Diene and Dienophile

DA reactions are second order reactions and, hence, depend on the concentrations of the diene and dienophile. In this method, the dienophile, enamine **7**, as well as the diene, the phthalazine-LA complex **A** are generated in situ by equilibrium reactions. Thermodynamic considerations of the $\Delta_r G$ values obtained from calculations indicate the status of these equilibria (Scheme 3). A $\Delta_r G$ value of $-6.4\ kcal \cdot mol^{-1}$ was calculated for the exergonic formation of the phthalazine-LA complex **A**. Conversely, computations on the formation of enamine **7b** gave a $\Delta_r G$ value of $1.3\ kcal \cdot mol^{-1}$. The amine-enamine equilibrium position is therefore located on the amine side with an amine/enamine ratio of 94:6. This observation corresponds to the fact that similar synthetic methods with enamine intermediates often require an excess of both amine and aldehyde to ensure a sufficient level of enamine concentration in the reaction mixture. However, using an excess of amine is not beneficial in the IEDDA/thiol transfer reaction described here, since secondary amines can react as exchange groups, which would generate the amine substituted by-product.[7c] Catalytic amine loadings of 20 mol% have been proven as a practical compromise between reaction time and the amount of side products formed. In addition, an aldehyde/amine ratio of 7.5:1.0 was found to be superior in the IEDDA/thiol transfer reaction. An aldehyde/amine mixture with this ratio was analyzed by ^{1}H NMR spectroscopy (see Supporting Information Figure S2). In this way, the starting materials were present in the same concentrations as in the IEDDA/thiol transfer reaction. The amine **6a** was not detectable in this experiment, because the equilibrium is shifted to the enamine **7a**, due to the 7.5-fold excess of aldehyde **2a**. The configuration of the enamine double bond is essential for the further course of the reaction. Comparison of calculated ΔG values showed that the *trans*-configuration is preferred in relation to the *cis*-isomer by $2.3\ kcal \cdot mol^{-1}$. Accordingly, enamine **7b** was identified in the ^{1}H NMR spectra only in its *trans*-configuration.

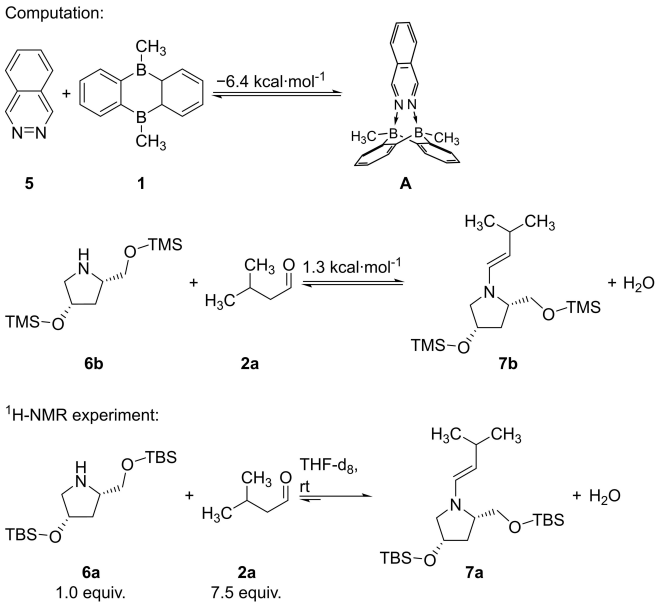

Scheme 3. Computational simulations and ^{1}H NMR experiment on the formation of enamine **7b** from secondary amine **6a** and isovaleraldehyde **2a** as well as the formation of phthalazine-Me_2-DBA complex **A**. The $\Delta_r G$ values were calculated on DLPNO-CCSD(T)/def2-tzvpp//M06-2x/def2-tzvpp (1 atm, 335 K) level of theory. ^{1}H NMR experiment: amine **6a** (20.5 µL, 50.0 µmol, 1.00 equiv.) and isovaleraldehyde **2a** (40.2 µL, 375 µmol, 7.50 equiv.) were dissolved in dry THF-d_8 (1.0 mL) and a ^{1}H NMR spectrum was measured.

The IEDDA Step

We demonstrated that the stereoselectivity of the method is unaffected by the choice of thiophenol used and concluded that the enantioselectivity is established in the IEDDA step.[6] The arrangement of the phthalazine-catalyst complex **A** and the enamine **7** in the IEDDA transition state control the course of this step. Due to the C_2 symmetry of the phthalazine-Me_2-DBA complex **A** enamine **7** can be arranged in four different orientations in both relevant sectors of the Me_2-DBA-phthalazine complex **A**. As discussed above, only the *trans*-isomer of the enamine is considered, resulting in the *trans*-arrangement of *iso*-propyl-group and amine. These four arrangements result in four different reaction pathways (Scheme 4), which were simulated separately by DFT computations. The relative Gibbs energy diagram is exemplary shown for pathway **IV** (Figure 1). Our investigations indicated similar trajectories for all four cases. Two separated activation barriers can be distinguished for each of the two C–C bond formations displaying a non-concerted pathway for the IEDDA step. In the first stage, the C–C bond between phthalazine and the C-atom of the enamine double bond with a larger orbital coefficient is formed, followed by the second C–C bond. The first barrier via **TS1** is higher in energy than the second one **TS2**, separated by a metastable intermediate **Int**. The overall reaction sequence is slightly exergonic. Similar observations have been made by us as well as others (e.g. Houk and co-workers for the IEDDA reaction of 1,2,3-triazines).[16]

The reaction pathway via **IV_TS1** and **IV_TS2** was found to be the lowest energy pathway (Table 1). This reaction corridor leads to the *o*-quinodimethane enantiomer **C-2**, which ultimately yields the (1*R*,2*S*)-enantiomer of product **4**.[6] Pleasingly, the computational results are consistent with experimental data, as (1*R*,2*S*)-enantiomer is also the main stereoisomer in the IEDDA/thiol group exchange reactions.

The Group Transfer Step

More than 20 different thiols, including aliphatic, heterocyclic and thiophenolic ones were screened in our initial study.[6]

Research Article
doi.org/10.1002/ejoc.202201289

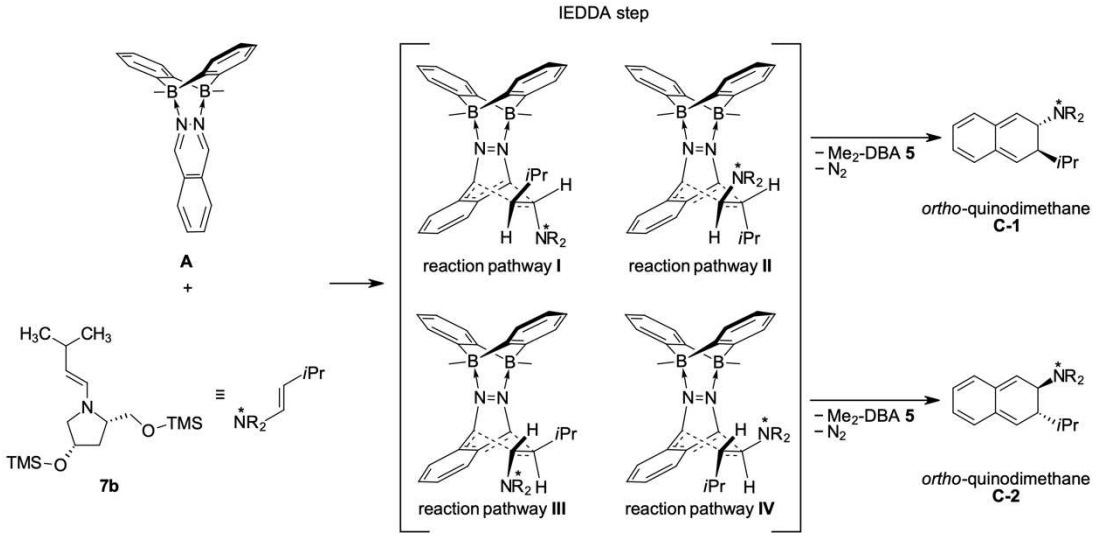

Scheme 4. Four arrangements of *trans*-enamine **7b** and phthalazine-LA complex **A** are possible in the IEDDA step. Each of these arrangements leads to a different reaction pathway and produces either *o*-quinodimethane enantiomer **C-1** or **C-2**.

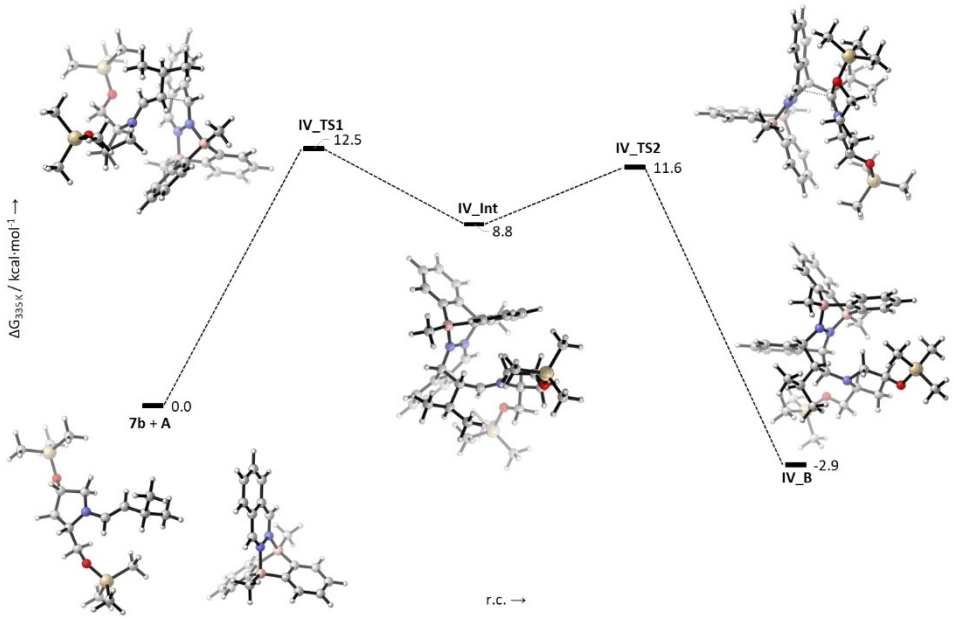

Figure 1. Relative Gibbs energy profile for the IEDDA reaction from enamine **7b** and intermediate **A** to product **B**. Structures were optimized at the M06-2x/def2-tzvpp level of theory (1 atm, 335 K) and energies were computed at DLPNO-CCSD(T)/def2-tzvpp.

Table 1. Relative Gibbs energy levels of stationary structures in the four potential reaction pathway **A** to **D**.

Entry	reaction pathway	$\Delta\Delta G_{335\,K}$[a]/kcal·mol^{-1}		
		TS1	Int	TS2
1	I	21.5	13.8	15.1
2	II	18.1	8.6	13.0
3	III	15.0	7.5	10.5
4	IV	12.5	8.8	11.6

[a] The $\Delta\Delta G_{335\,K}$ values were calculated on DLPNO-CCSD(T)/def2-tzvpp//M06-2x/def2-tzvpp (1 atm, 335 K) level of theory.

Thereby, thiophenols with different substitution patterns were investigated including the effect of *ortho*-, *meta*- and *para*-position. In the case of chlorothiophenols for all isomers a similar outcome was observed. Hence, we concentrated in the current study on *para*-substituted thiophenols (Table 2). Substrates with electron-withdrawing moieties, inclusive unsubstituted thiophenol (**3d**), gave moderate to good yields of the final thioether products **4** (entry 1–4), while with 4-methylthiophenol (**3e**) the elimination product **8** was formed (entry 5). This notable result can be explained by the proposed

Research Article
doi.org/10.1002/ejoc.202201289

Chemistry Europe
European Chemical Societies Publishing

Table 2. Scope of *para*-substituted thiophenoles. The entries are sorted by increasing nucleophilicity of the corresponding thiophenolate.[17]

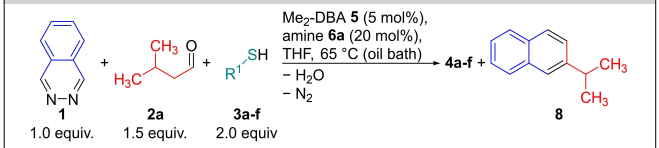

Entry	Thiophenol **3a–f**	Yield **4a–f**[a,b]	Yield **8**[a]
1	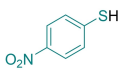	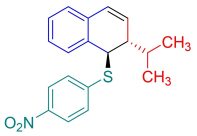	0%
2	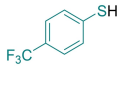	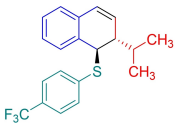	0%
3	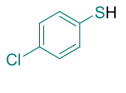	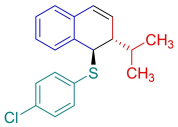	0%
4		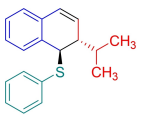	0%
5	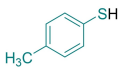	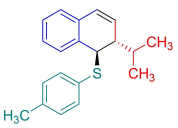	51%
6	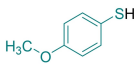	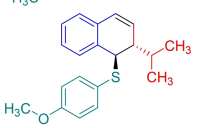	0%

Reaction conditions: phthalazine (**1**) (1.0 mmol, 1.0 equiv.), isovaleraldehyde (**2a**) (1.5 mmol, 1.5 equiv.), thiol (2.0 mmol, 2.0 equiv.), dry THF (4.0 mL). [a] Given yields are after purification by column chromatography. [b] E.r.s were determined by chiral HPLC.

mechanism of the group transfer step and the frontier molecule orbital (FMO) analysis given later in this article.

The IEDDA/group transfer reaction with 4-methoxythiophenol (**3f**) as exchange group proceeds atypically, because none of the expected products **4f** or **8** were observed and phthalazine (**1**) was not consumed in the presence of this thiophenol (Table 2, entry 6). Obviously, the IEDDA steps did not proceed and we speculated that either the formation of phthalazine-LA complex **A** or enamine **7a** was intercepted as soon as 4-methoxythiophenol (**3f**) is present in the reaction mixture. Thiols are nucleophiles, but also Lewis bases. As such, they might bind to the boron catalyst **5** and affect the formation of phthalazine-Me_2-DBA complex **A**, the activated diene. The influence of 4-methoxythiophenol (**3f**) on the formation of the BDLA-phthalazine complex **A** was investigated via a NMR experiment. For this purpose, a 1:1 mixture of phthalazine (**1**, 1.0 equiv.) and Me_2-DBA **5** (1.0 equiv.) was prepared in THF-d8. Then, 4-methoxythiophenol (**3f**, 2.0 equiv.) was added and a ^{1}H NMR spectrum was measured. No signals in this spectrum could be assigned to a complexation between 4-methoxythiophenol (**3f**) and Me_2-DBA **5**. Hence, an influence on the formation of the activated diene **A** could be excluded. Much more likely, 4-methoxythiophenol (**3f**) influences the formation of enamine **7**. In one way, 4-methoxythiophenol (**3f**) could react with isovaleraldehyde (**2a**) to form a dithioacetal. Nevertheless, with two equivalents of thiol, as it was used in the standard procedure a maximum of one equivalent aldehyde is abstracted from the reaction mixture, but 0.50 equivalents of aldehyde would remain to form enamine **7** together with secondary amine **6**. In this way, the IEDDA reaction would be slowed down, but not completely prevented. Since no thiophenol is then available for the group exchange step, amines are eliminated form intermediate **C**. In this situation, the main product is naphthalene **8**, as it is formed, for example, when 4-methylthiophenol (**3d**) is used. Interestingly, when mixtures of thiophenol (**3d**) and 4-methoxythiophenol (**3f**) in different ratios were subjected to the BiLa-catalyzed IEDDA/thiol transfer reaction phthalazine (**1**) was also not consumed (Scheme 5).

The fact, that even 0.5 equivalents of thiol **3f** are sufficient to inhibit the IEDDA step made the formation of a *N*,*S*-acetal from the enamine and the thiol more feasible. To verify this possibility, enamine **7c** was prepared as a test system (Scheme 6). Enamine **7c** and 4-methxythiophenol (**3f**) were then dissolved in a 1:1 ratio in THF-d8 and analyzed by ^{1}H NMR spectroscopy. It revealed, that enamine **7c** was completely converted to the *N*,*S*-acetal **10**. Hence, we can conclude that this method is limited by the nucleophilic character of the employed thiol. If the thiol is too nucleophilic, it converts the enamine more rapidly in a side reaction to the *N*,*S*-acetal, which prevents the intended IEDDA step.

Furthermore, the mechanism of the group transfer step was studied using computations. The reaction pathway for each of the *para*-substituted thiophenols **3a** to **3f** were calculated and is exemplarily shown for thiophenol (**3d**) with intermediate **C** (Figure 2). In a concerted process, first the acidic proton of the thiol is transferred to the amine group of intermediate **C**. This is followed by the nucleophilic attack of the thiophenolate on the

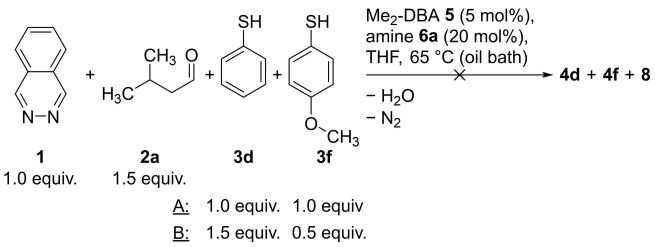

Scheme 5. Two IEDDA/thiol transfer reactions with mixtures of thiophenol (**3d**) and 4-methoxythiophenol (**3f**) in different ratios. All other reaction conditions were maintained compared to the standard procedure. Experimental details: phthalazine (**1**) (131 mg, 1.00 mmol, 1.00 equiv.), isovaleraldehyde (**2a**) (161 µL, 1.50 mmol, 1.50 equiv.), A: thiophenol (**3d**) (104 µL, 1.00 mmol, 1.00 equiv.), 4-methoxythiophenol (**3f**) (123 µL, 1.00 mmol, 1.00 equiv.), B: thiophenol (**3d**) (156 µL, 1.50 mmol, 1.50 equiv.), 4-methoxythiophenol (**3f**) (61.5 µL, 500 µmol, 0.500 equiv.), Me_2-DBA **5** (10.2 mg, 50.0 µmol, 5.00 mol%), chiral amine **6a** (81.8 µL, 200 µmol, 20.0 mol%) dry THF (4.0 mL), 65 °C, 12 days. Conversion of phthalazine (**1**) was followed by ^{1}H NMR. In both experiments, no phthalazine (**1**) was converted.

Research Article
doi.org/10.1002/ejoc.202201289

Chemistry Europe
European Chemical Societies Publishing

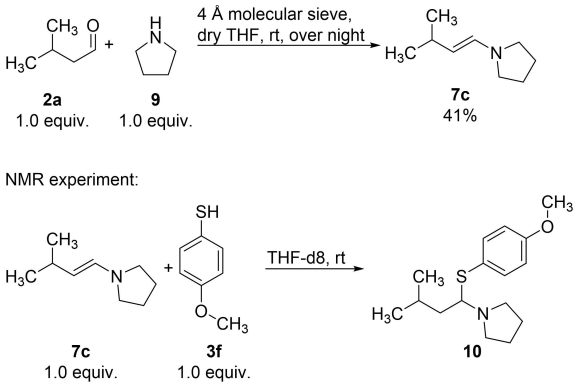

Scheme 6. Preparation of enamine **7c** as a test system to investigate the formation of *N,S*-acetal **10**. Experimental details on synthesis of **7c**: isovaleraldehyde (**2a**) (1.07 mL, 10.0 mmol, 1.00 equiv.), pyrrolidine (**9**) (0.821 mL, 10.0 mmol, 1.00 equiv.), dry THF (20 mL), five pellets of molecular sieve. Crude enamine **7c** was purified by distillation (55 °C, 4.0 mbar). NMR experiment: Enamine **7c** (157 µL, 1.00 mmol, 1.00 equiv.), 4-methoxythiophenol **3f** (123 µL, 1.00 mmol, 1.00 equiv.) were dissolved in dry THF-d8 (2.0 mL). The mixture was stirred for 30 min at 65 °C, then 1.0 mL was transferred to a NMR-tube and a ^{1}H NMR spectrum was measured. The enamine double bond signals at 4.00 ppm (dd) and 6.09 ppm (d) were completely quenched.

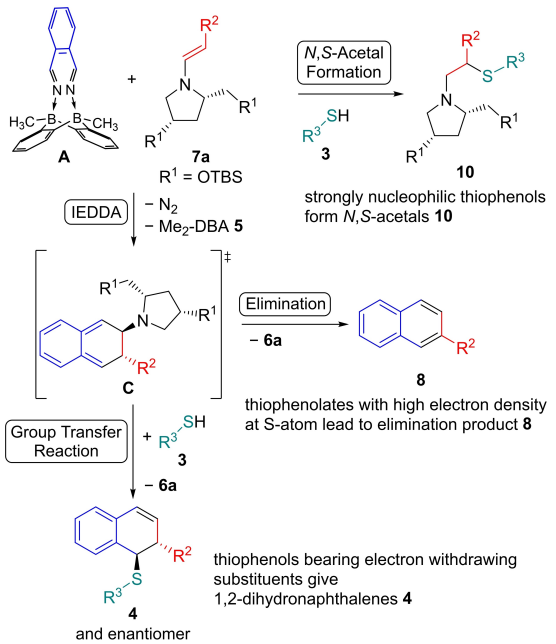

Scheme 7. Thiophenols with different nucleophilic potential lead to different products in the course of the reaction. Three different situations were traced: The formation of N,S-acetals, the elimination and the product forming process.

carbon atom with simultaneous cleavage of the secondary amine. A separation of thiophenolate and protonated intermediate **C** after the proton has been transferred is rather unlikely, because the calculated barrier is approximately 90 kcal·mol^{-1}. This conclusion is supported by experimental data. Since *syn*-1,2-dihydronaphthalenes might be formed

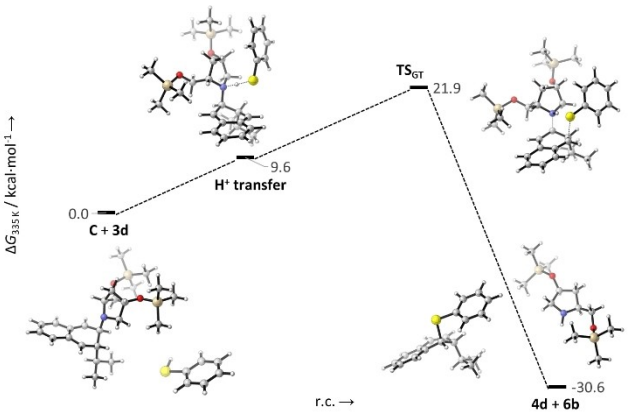

Figure 2. Relative Gibbs energy profile for the group transfer reaction from intermediate **C** and thiophenol (**3d**) to product **4d**. Structures were optimized at the M06-2x/def2-tzvpp level of theory (1 atm 335 K), and energies were computed at DLPNO-CCSD(T)/def2-tzvpp.

when these ions are separated. However, *syn*-products were not found in any of the executed IEDDA/thiol transfer experiments.

The calculated $\Delta\Delta G^{\ddagger}$ values and the C-S distances in the TS_{GT} increase proportionally with the increasing nucleophilicity of the corresponding thiophenolates in the series of *para*-substituted thiophenols **3a** to **3f** (Table 3). To illuminate this assessment, the FMOs of the thiophenolates **E** to **J** and the protonated intermediate **D** were calculated at ωB97X-D/cc-pVTZ level of theory (Figure 3).[18] The representative FMOs are exemplified by thiophenolate. Qualitative analysis of the FMOs indicated, that the overlap of HOMO-$1_{thiolate}$ and $LUMO_D$ is the most relevant attractive orbital interaction. This is countered by repulsion between HOMO-$1_{thiolate}$ and $HOMO_D$. The p_y-orbital of the S-atom is the major contributor to HOMO-$1_{thiolate}$.

In the series of thiophenolates **E** to **J**, the electron density at the S-atom increases. Along with this the orbital coefficient of the p_y-orbital becomes larger and HOMO-1 gets bulkier. But the sequential larger orbital overlap between HOMO-$1_{thiolate}$ and $LUMO_D$ is overcompensated by repulsion between HOMO-$1_{thiolate}$ and $HOMO_D$, causing higher $\Delta\Delta G^{\ddagger}$ values and larger C-S distances in the TS_{GT} (Table 4).

Table 3. Relative energy levels of the activation barriers and C-S distances in the transition states of the group transfer reactions with different *para*-thiophenols.[a]

Entry	Thiophenol	$\Delta\Delta G^{\ddagger}$ /kcal·mol^{-1}	C-S-distance /Å
1	4-nitro-thiophenol **3a**	19.9	2.30
2	4-(trifluoromethyl)-thiophenol **3b**	21.0	2.34
3	4-chloro-thiophenol **3c**	21.9	2.36
4	thiophenol **3d**	21.9	2.39
5	4-methylthiophenol **3e**	22.9	2.41
6	4-methoxythiophenol **3f**	22.4	2.42

[a] Geometries were optimized at the M06-2x/def2-tzvpp level of theory (1 atm, 335 K), and energies were computed at DLPNO-CCSD(T)/def2-tzvpp.

Research Article
doi.org/10.1002/ejoc.202201289

Chemistry Europe
European Chemical Societies Publishing

Table 4. Charge densities at the S-atom in the series of thiophenolates **E** to **J**.[a]

Entry	Thiophenolate	Charge density at S
1	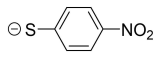 **E**	−0.589
2	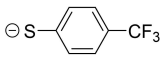 **F**	−0.651
3	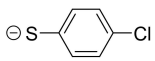 **G**	−0.682
4	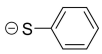 **H**	−0.702
5	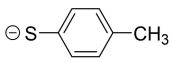 **I**	−0.710
6	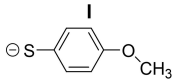 **J**	−0.724

[a] Charge densities were calculated at ωB97X–D/cc-pVTZ (335 K, 1 atm) level of theory.

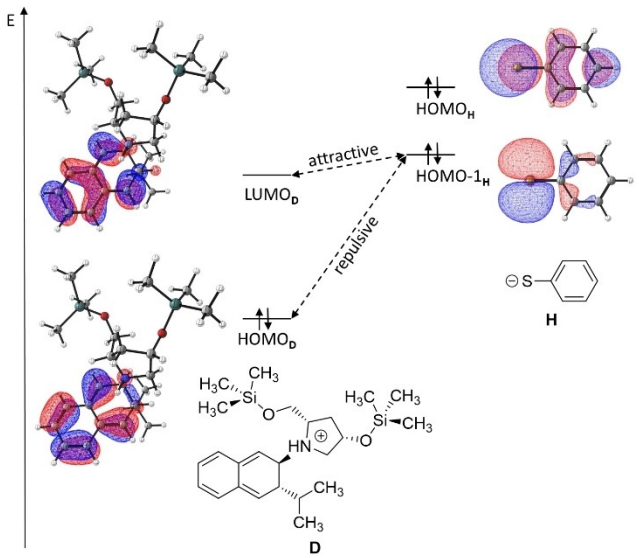

Figure 3. The leading frontier molecule orbitals in the group transfer step. $LUMO_D$ and $HOMO_D$ of intermediate **C** are depicted at the left site and the HOMO-1 of thiophenolate **H** at the right site. The molecular orbitals are calculated at ωB97X–D/cc-pVTZ (335 K, 1 atm) level of theory. Attractive interactions are developed between HOMO-1_H and $LUMO_D$. They are counteracted by repulsive interactions between HOMO-1_H and $HOMO_D$, as they are not in phase.

Conclusion

Herein we presented detailed studies on the mechanism of our recently developed MCR, the enantioselective bidentate Lewis acid catalyzed domino inverse electron-demand Diels-Alder/thiol transfer reaction accessing potentially bioactive thioether substituted 1,2-dihydronaphthalenes. The process can be divided in three parts, the formation of the active diene and dienophile, the IEDDA step and the final groups transfer. In particular, we wanted to understand why thiols, which represent supposedly better nucleophile do not automatically lead to better yields or higher reaction rates (Scheme 7). In fact, thiols with strong nucleophilic character do not convert to the expected products at all. We demonstrated, that the use of such thiol interrupts enamine-based reaction processes. Instead, *N,S*-acetals are formed. In the IEDDA key step the enantioselectivity is determined. In the present process this step proceeds though a stepwise mechanism. In addition, we were able to locate a plausible arrangement of the enamine and phthalazine-LA complex resulting in the main enantiomer of the thioether product. FMO analysis of the group exchange reaction showed that a higher electron density at the sulfur atom leads to a larger reaction barrier of the exchange step. This makes the elimination reaction more likely compared to the thiol exchange reaction and explains the formation of product **8** when 4-methylthiophenol (**3e**) is used as exchange component. Understanding the mechanism of this process will provide valuable knowledge to design other novel MCRs. In general, detailed insights into chemical processes improve our understanding of how structure is related to reactivity.

Experimental Section

Standard procedure of the IEDDA/group transfer reaction:[6] In a nitrogen filled glovebox phthalazine (**1**) (131 mg, 1.00 mmol, 1.00 equiv.) and Me_2-DBA **5** (10.2 mg, 5.00 mol, 5.00 mol%) were suspended in dry THF (4 mL). Then, isovaleraldehyde (**2a**) (161 µL, 1.50 mmol, 1.50 equiv.) was added and the reaction vessel was sealed. The reaction set-up was continued under Schlenk conditions outside the glovebox. Afterwards, thiophenol **3** (2.00 mmol, 2.00 equiv.) was added, followed by amine **6b** (81.8 µL, 20.0 µmol, 20.0 mol%). The bright yellow suspension was stirred at 65 °C (oil bath) for several days. The reaction progress was monitored by ^{1}H NMR. After full conversion of phthalazine (**1**) the mixture was concentrated under reduced pressure. An orange oil was obtained. The crude product was purified by flash column chromatography (silica gel) and was isolated as a colorless oil. The enantiomeric ratio was determined by chiral HPLC.

Further experimental data like characterizations, original spectra, etc., is provided in the Supporting Information.

Acknowledgements

Calculations for this research were conducted on the "Fuchs" high performance computer of the Goethe University Frankfurt. The authors thank the German Research Council (Deutsche Forschungsgemeinschaft, DFG) for funding. Open Access funding enabled and organized by Projekt DEAL.

Conflict of Interest

The authors declare no conflict of interest.

Research Article
doi.org/10.1002/ejoc.202201289

Data Availability Statement

The data that support the findings of this study are available in the supplementary material of this article.

Keywords: Lewis acid catalysis · domino processes · Diels-Alder reaction · mechanistic studies · multicomponent reaction

[1] Y. Hayashi, *J. Org. Chem.* **2021**, *86*, 1–23.
[2] B. Ganem, *Acc. Chem. Res.* **2009**, *42*, 463–472.
[3] a) H. Wehlan, J. Oehme, A. Schäfer, K. Rossen, *Org. Process Res. Dev.* **2015**, *19*, 1980–1986; b) H. Liu, S. William, E. Herdtweck, S. Botros, A. Dömling, *Chem. Biol. Drug Des.* **2012**, *79*, 470–477; c) C. Kalinski, H. Lemoine, J. Schmidt, C. Burdack, J. Kolb, M. Umkehrer, G. Ross, *Synthesis* **2008**, *2008*, 4007–4011; d) S. Malaquin, M. Jida, J.-C. Gesquiere, R. Deprez-Poulain, B. Deprez, G. Laconde, *Tetrahedron Lett.* **2010**, *51*, 2983–2985; e) A. Znabet, M. M. Polak, E. Janssen, F. J. J. de Kanter, N. J. Turner, R. V. A. Orru, E. Ruijter, *Chem. Commun.* **2010**, *46*, 7918–7920; f) I. Aillaud, C. Haurena, E. Le Gall, T. Martens, G. Ricci, *Molecules* **2010**, *15*, 8144–8155; g) H. Farhid, V. Khodkari, M. T. Nazeri, S. Javanbakht, A. Shaabani, *Org. Biomol. Chem.* **2021**, *19*, 3318–3358.
[4] D. Insuasty, J. Castillo, D. Becerra, H. Rojas, R. Abonia, *Molecules* **2020**, *25*, 505.
[5] a) Y. E. Türkmen, T. J. Montavon, S. A. Kozmin, V. H. Rawal, *J. Am. Chem. Soc.* **2012**, *134*, 9062–9065; b) T. J. Montavon, Y. E. Türkmen, N. A. Shamsi, C. Miller, C. S. Sumaria, V. H. Rawal, S. A. Kozmin, *Angew. Chem. Int. Ed.* **2013**, *52*, 13576–13579; *Angew. Chem.* **2013**, *125*, 13821–13824; c) C. S. Sumaria, Y. E. Türkmen, V. H. Rawal, *Org. Lett.* **2014**, *16*, 3236–3239; d) Q. Chen, M. Luo, F. Guo, K. Liang, F. Zhou, G. Gao, *Adv. Synth. Catal.* **2020**, *362*, 2332–2336; e) Q. Chen, X. Zheng, F. Guo, K. Liang, F. Zhou, *J. Org. Chem.* **2021**, *86*, 18278–18286.
[6] S. Beeck, S. Ahles, H. A. Wegner, *Chem. Eur. J.* **2022**, *28*, e202104085.
[7] a) S. N. Kessler, M. Neuburger, H. A. Wegner, *Eur. J. Org. Chem.* **2011**, *2011*, 3238–3245; b) L. Schweighauser, I. Bodoky, S. N. Kessler, D. Häussinger, C. Donsbach, H. A. Wegner, *Org. Lett.* **2016**, *18*, 1330–1333; c) S. Ahles, S. Götz, L. Schweighauser, M. Brodsky, S. N. Kessler, A. H. Heindl, H. A. Wegner, *Org. Lett.* **2018**, *20*, 7034–7038; d) J. Ruhl, S. Ahles, M. A. Strauss, C. M. Leonhardt, H. A. Wegner, *Org. Lett.* **2021**, *23*, 2089–2093; e) S. Ahles, J. Ruhl, M. A. Strauss, H. A. Wegner, *Org. Lett.* **2019**, *21*, 3927–3930.
[8] a) S. Mukherjee, J. W. Yang, S. Hoffmann, B. List, *Chem. Rev.* **2007**, *107*, 5471–5569; b) A. Gualandi, L. Mengozzi, C. M. Wilson, P. G. Cozzi, *Chem. Asian J.* **2014**, *9*, 984–995.
[9] D. E. Fogg, E. N. dos Santos, *Coord. Chem. Rev.* **2004**, *248*, 2365–2379.
[10] A. Lorbach, M. Bolte, H.-W. Lerner, M. Wagner, *Chem. Commun.* **2010**, *46*, 3592–3594.
[11] S. N. Kessler, H. A. Wegner, *Org. Lett.* **2010**, *12*, 4062–4065.
[12] a) N. Mardirossian, M. Head-Gordon, *Mol. Phys.* **2017**, *115*, 2315–2372; b) L. Goerigk, A. Hansen, C. Bauer, S. Ehrlich, A. Najibi, S. Grimme, *Phys. Chem. Chem. Phys.* **2017**, *19*, 32184–32215.
[13] M. Linder, T. Brinck, *Phys. Chem. Chem. Phys.* **2013**, *15*, 5108–5114.
[14] S. Grimme, J. Antony, S. Ehrlich, H. Krieg, *J. Chem. Phys.* **2010**, *132*, 154104.
[15] N. Mardirossian, M. Head-Gordon, *J. Chem. Theory Comput.* **2016**, *12*, 4303–4325.
[16] a) M. A. Strauss, D. Koh, J. Ruhl, H. A. Wegner, *Eur. J. Org. Chem.* **2021**, *2021*, 3866–3873; b) Ö. N. Avcı, S. Catak, B. Dereli, V. Aviyente, B. Dedeoglu, *ChemCatChem* **2020**, *12*, 366–372; c) Y.-F. Yang, P. Yu, K. N. Houk, *J. Am. Chem. Soc.* **2017**, *139*, 18213–18221; d) P. Vermeeren, T. A. Hamlin, F. M. Bickelhaupt, *Phys. Chem. Chem. Phys.* **2021**, *23*, 20095–20106.
[17] P. M. Jüstel, C. D. Pignot, A. R. Ofial, *J. Org. Chem.* **2021**, *86*, 5965–5972.
[18] T. Tsuneda, K. Hirao, *WIREs Comput. Mol. Sci.* **2014**, *4*, 375–390.

Manuscript received: November 1, 2022
Revised manuscript received: December 2, 2022
Accepted manuscript online: December 7, 2022